Green Chemistry

PAPER

Understanding the role of co-solvents in the dissolution of cellulose in ionic liquids†

Cite this: *Green Chem.*, 2014, **16**, 2528

Jean-Michel Andanson,[a,b] Emilie Bordes,[a,b] Julien Devémy,[a,b] Fabrice Leroux,[a,b] Agilio A. H. Pádua[a,b] and Margarida F. Costa Gomes*[a,b]

The dissolution of microcrystalline cellulose in 1-butyl-3-methylimidazolium acetate [C_4C_1Im][OAc] was studied using a solid–liquid equilibrium method based on polarized-light optical microscopy from 30 to 100 °C. We found that [C_4C_1Im][OAc] could dissolve as much as 25 wt% of cellulose at temperatures below 100 °C. The structure of the composite phase obtained after cooling a solution of 16 wt% of cellulose in [C_4C_1Im][OAc] was analyzed by low angle X-ray diffraction showing the absence of microcrystalline cellulose, but depicting an extensive long range isotropic ordering. With the aim of improving the dissolution of cellulose in the ionic liquid, dimethyl sulfoxide, DMSO, was added as a co-solvent. It was observed that it enhances the solvent power of the ionic liquid by decreasing the time needed for dissolution, even at low temperatures. In order to understand what makes DMSO a good co-solvent, two approaches were followed. Firstly, we studied experimentally the mass transport properties (viscosity and ionic conductivity) of [C_4C_1Im][OAc] + DMSO mixtures at different compositions and, secondly, we assessed the molecular structure and interactions around glucose, the structural unit of cellulose, by means of molecular dynamics simulations. As expected, DMSO dramatically decreases the viscosity and increases the conductivity of the mixtures, but without inducing cation–anion dissociation in the ionic liquid. These results were confirmed by molecular simulation as it was found that the presence of a 0.5 mole fraction concentration of DMSO does not significantly affect the hydrogen-bond network in the ionic liquid. Furthermore, molecular dynamics shows that in the [C_4C_1Im][OAc] + DMSO equimolar mixture, DMSO does not interact specifically with glucose. We conclude that DMSO improves the solvation capabilities of the ionic liquid because it facilitates mass transport by decreasing the solvent viscosity without significantly affecting the specific interactions between cations and anions or between the ionic liquid and the polymer. The behavior of DMSO as a co-solvent was compared with that of water and it was found that water molecules are more probably found near glucose than those of DMSO, thus interfering with ionic liquid–glucose interactions, which might explain the unsuitability of water as a co-solvent for cellulose in ionic liquids.

Received 31st October 2013,
Accepted 28th January 2014

DOI: 10.1039/c3gc42244e

www.rsc.org/greenchem

1. Introduction

Cellulose is a cheap and abundant natural polymer that has numerous applications.[1] In many of these applications, the polymer has first to be dissolved.[2] Natural cellulose is a crystalline biopolymer composed of monomers of cellobiose (2 glucose molecules linked by a β(1–4) bond) each having six OH groups that give rise to a strong hydrogen-bond network, both intra- and intermolecular. These specific interactions make natural cellulose a thermally and chemically stable material that is very difficult to solubilize.

Dissolving natural cellulose is a demanding task since water or the usual organic solvents are not able to dissolve this polymer under relatively mild conditions. The industrial processes currently in use are hazardous and should be replaced mainly because of environmental reasons.[3] In 2002, Swatloski *et al.*[4] reported that ionic liquids could dissolve cellulose efficiently. These are thermally stable, non-volatile fluids which might decrease the risk of pollution and facilitate recycling.[5] Over the last ten years, numerous ionic liquids have been tested for cellulose dissolution.[6] Those based on acetate anions and alkylimidazolium cations were proved to dissolve high amounts of cellulose at temperatures below 100 °C[7–11] (>15 wt% after a few hours at 100 °C)[9] with the advantage,

[a]*Clermont Université, Université Blaise Pascal, Institut de Chimie de Clermont-Ferrand, BP 10448, F-63000 Clermont-Ferrand, France.*
E-mail: margarida.c.gomes@univ-bpclermont.fr
[b]*CNRS, UMR 6296, ICCF, F-63171 Aubiere, France*

†Electronic supplementary information (ESI) available. See DOI: 10.1039/c3gc42244e

contrary to chloride alkylimidazolium ionic liquids, of being liquid at room temperature.

Leitner *et al.* compared the ability of 17 carboxylate-based ionic liquids to dissolve 1 wt% of cellulose by adding progressively 1 wt% of biomass every 30 min at a given temperature to determine the solubility of the biopolymer.[9] Ionic liquids are generally highly viscous,[12,13] and adding a polymer into a solvent is known to increase even more the viscosity of the liquid.[14–16] Because of this, the dissolution of high amounts of cellulose in an ionic liquid can be limited by mass transport and not only by unfavorable solute–solvent interactions. Seddon *et al.*[17] followed the kinetics of dissolution of 10 wt% of cellulose using viscosity measurements thus contributing, with an original experimental protocol, to a better understanding of the mechanisms of dissolution of cellulose in ionic liquids.[18]

The addition of highly polar and aprotic co-solvents to ionic liquids has proven to considerably improve cellulose dissolution.[19,20] Several solvents were tested and dimethyl sulfoxide, DMSO, a strongly polar (μ = 3.96 D) aprotic organic liquid with a high boiling point (189 °C) and a good thermal stability, appears to be a good co-solvent. The addition of a co-solvent induces an exponential decrease of the viscosity of the polymer solutions as recently observed for DMSO[21] or carbon dioxide.[22] Because mass transfer is improved, the temperature at which the dissolution of a given concentration of polymer is observed might be lower. This should constitute an advantage in terms of recyclability when using ionic liquids such as 1-butyl-3-methylimidazolium acetate, [C_4C_1Im][OAc], which decomposes by 1% within 10 h at 102 °C.[23]

Here we report the study of cellulose dissolution in [C_4C_1Im][OAc] and in [C_4C_1Im][OAc] + DMSO mixtures. To study the dissolution of the polymer, we used a synthetic (global composition) phase equilibrium method with visual detection by polarized-light optical microscopy, an easily accessible technique especially useful to study microcrystalline cellulose (MCC) in ionic liquids.[24,25] The first original approach of this work concerns the accurate determination of the dissolution conditions (temperature, concentration and time) of well-characterized commercial samples of microcrystalline cellulose. To the best of our knowledge, only one study of the kinetics of cellulose dissolution in ionic liquids has been reported using viscosity measurements.[17] In order to understand the effect of DMSO on the polymer solvation, we have studied the properties of the ionic liquid + DMSO mixtures both experimentally and by molecular dynamics simulation. Experimentally, we determined the viscosity and conductivity of the mixtures and calculated their "ionicity" in order to evaluate the effect of the molecular solvent on the cation–anion interactions in the ionic liquid.[26] Molecular dynamics simulations were performed both of the [C_4C_1Im][OAc] + DMSO mixtures and of the solutions of glucose (the basic structural unit of cellulose) in those mixtures. The microscopic structure and the molecular interactions in solution were analyzed. The association of simple macroscopic measurements with molecular simulation studies to assess the molecular interactions in the solutions of cellulose constitutes the second original approach of the present work.

2. Methodology

2.1. Materials

[C_4C_1Im][OAc] from Interchem (98%) was used without further purification. The amount of water of the ionic liquid freshly purchased was 0.6 wt%. Because [C_4C_1Im][OAc] is highly hygroscopic and it was very difficult to keep it under a dry atmosphere during the experiments, we have performed all the measurements in an ionic liquid with a controlled quantity of water of 1 wt%. We have avoided in this way the change in the properties of the ionic liquid (in particular of its viscosity) due to an uncontrolled absorption of water. DMSO (dimethyl sulfoxide, >99.9%, from Fluka) was used as a co-solvent. [C_4C_1Im][OAc] + DMSO mixtures with mole fraction concentrations in ionic liquid of x_{IL} = 0.25, 0.50 and 0.75 were prepared gravimetrically. Cellulose (microcrystalline cellulose from Sigma-Aldrich) was dried in an oven at 90 °C for 1 day prior to usage.

2.2. Experimental

A small amount of cellulose suspension was prepared by adding 50 mg of [C_4C_1Im][OAc] (or [C_4C_1Im][OAc] + DMSO mixture) to a known amount of cellulose on a glass slide. The suspension was quickly stirred before closing the sample with a glass coverslip. The overall compositions of cellulose given in this paper refer to the mass ratio of cellulose over the mass of solvent (ionic liquid + co-solvent), %wt = 100 × ($m_{cellulose}$/$m_{solvent}$). The sample of cellulose suspension was then placed in the hot stage (Linkam LTS420) of the optical microscope (Leica DM2500M) preheated at 30.0 °C.

Changes in the sample when it was heated at rates of 1.0, 0.1 or 0.01 °C min^{-1} were followed in the microscope *via* cross-polarized light, which is specifically sensitive to the crystalline part of the sample. In a typical experiment, the sample was heated from 30.0 to over 100.0 °C and an image (2048 × 1536 pixels) was recorded every 0.5 °C. Some experiments were also conducted at constant temperature. The area observed in the microscope is of 900 × 1200 μm while the whole sample area is of approximately 4 cm^2. During the experiment, the hot stage containing the sample is flushed with N_2 to avoid any water uptake, especially for the longest experiments that take several days.

The electrical conductivity, κ, was measured with the ac impedance bridge technique using two platinum electrodes. Details of our setup can be found elsewhere.[27] Viscosity measurements were performed with an Anton Paar AMVn rolling ball viscosimeter. The overall uncertainty in the viscosity is estimated as ±1.5%.[27] In order to calculate the viscosity of the sample using a rolling ball viscosimeter, the density of the sample has to be known. Densities of all samples were also measured for all temperatures with a DMA 5000M vibrating-tube densimeter from Anton Paar. Conductivity and viscosity of the [C_4C_1Im][OAc] + DMSO mixtures were

measured at compositions x_{IL} = 0.0, 0.25, 0.50, 0.75 and 1.0, from 25.0 to 100.0 °C.

X-ray diffraction analysis, XRD, of the composite sample cellulose + ionic liquid was performed at room temperature on a Siemens D501 diffractometer in a Bragg–Brentano θ–2θ configuration using a Cu Kα source (25 mA, 35 kV). Data were collected in a step scan mode between 0.7 and 28.0° (2θ) with a step size of 0.005° and a counting time of 9 s per step. The slits before and after the sample were close to 0.3°. The solution analyzed was prepared as described above with a concentration of 16.2 wt% of cellulose in [C_4C_1Im][OAc]. After dissolution, the sample was left at room temperature under a nitrogen atmosphere for 48 h before the X-ray measurement. The Bragg relationship was used to access the distance values d as λ(Å) = $2d\sin\theta$, where λ and θ are the wavelength (here 1.5418 Å) and the diffracting angle, respectively. The instrumental full width at half maximum (FWHM) was not considered here at such low 2θ values when using the Scherrer relation

$$L = \frac{0.9 \times \lambda}{\sqrt{\Delta\theta_m^2 - \Delta\theta_0^2}} \times \frac{1}{\cos\theta}$$

where L is the size of the coherent domain visualized by X-ray, $\Delta\theta_m^2$ is the full width at half maximum (FWHM) of the diffraction line, $\Delta\theta_0^2$ is the instrumental FWHM (here not considered) and λ is the wavelength. The sample was observed by the optical microscope under polarized light before and after the diffraction analysis.

2.3. Molecular simulation

Flexible all-atom models of the OPLS-AA family were used for [C_4C_1Im][OAc],[28–30] glucose,[31] DMSO,[28] and water (TIP4P)[32] molecules. Their chemical structures are represented in Fig. 1. Simulations were performed in periodic cubic boxes containing 512 ion pairs (or 1024 ion pairs if no co-solvent), using the molecular dynamics method implemented in the DL_POLY package.[33] Equimolar mixtures of [C_4C_1Im][OAc] with 512 molecules of DMSO or water were also simulated. Systems including sixteen glucose molecules were simulated in order to study the microscopic structure and the molecular interactions of the solvent around the structural unit of cellulose. The composition of the different simulated systems is summarised in ESI.† Once the equilibrium density was achieved, simulation runs of 400 ps were performed in the NPT ensemble at 150 °C and 1 bar (5 bar in the case of water as a co-solvent), maintained by the Nosé–Hoover thermostat and barostat. The time step used was 2 fs and the cutoff distance was 16 Å for non-bonded interactions. Long-range electrostatic interactions were handled by the Ewald summation method with an accuracy of 10^{-4}. Structural quantities such as radial distribution functions and hydrogen bond statistics were calculated from configurations saved every 2 ps. H-bonds were defined using standard geometric criteria of distance and angle: H···O distance under 2.5 Å and O–H···O angle between 150° and 180°; for the weaker C–H···O bond involving the aromatic ring of the cation, a longer distance of 3.0 Å was necessary (see radial distribution functions below). Similar parameters were used for the study of cellulose–[C_2C_1Im]-[OAc]–water ternary mixtures.[34]

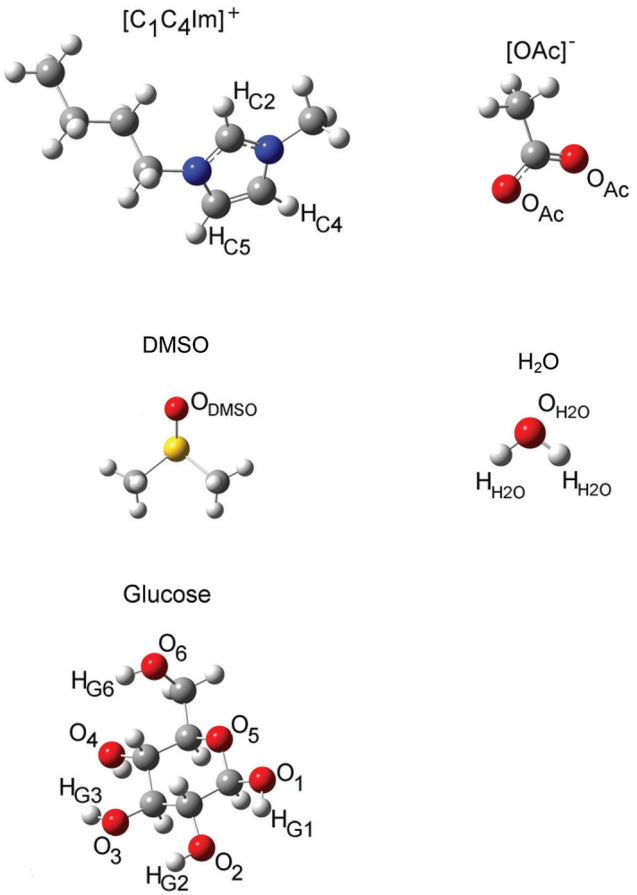

Fig. 1 Adopted nomenclature for the sites of the ionic liquid 1-butyl-3-methylimidazolium acetate ([C_4C_1Im][OAc]), dimethyl sulfoxide (DMSO), water and glucose.

3. Results and discussion

Typical images of the cellulose dissolution in [C_4C_1Im][OAc] are shown in Fig. 2. In these images, white spots correspond to the crystalline cellulose fibres, which disappear with time. Dissolution experiments were explored by evaluating automatically all images using a home-made software that analyses the brightness of each image and plots it as a function of time during the experiment. Examples of measurements are represented in Fig. 3 for three mass concentrations of cellulose in [C_4C_1Im][OAc] at 50 °C. At the lower concentration of 5 wt%, cellulose is dissolved in less than 2 hours, while at 10 wt% it is still slowly dissolving after 10 hours and for 20 wt% of cellulose the polymer is not fully dissolved in the ionic liquid at this temperature. For the 10 wt% concentration, it is observed in Fig. 3 that the brightness first decreases (corresponding to the disappearance of the crystals of cellulose seen in white, see

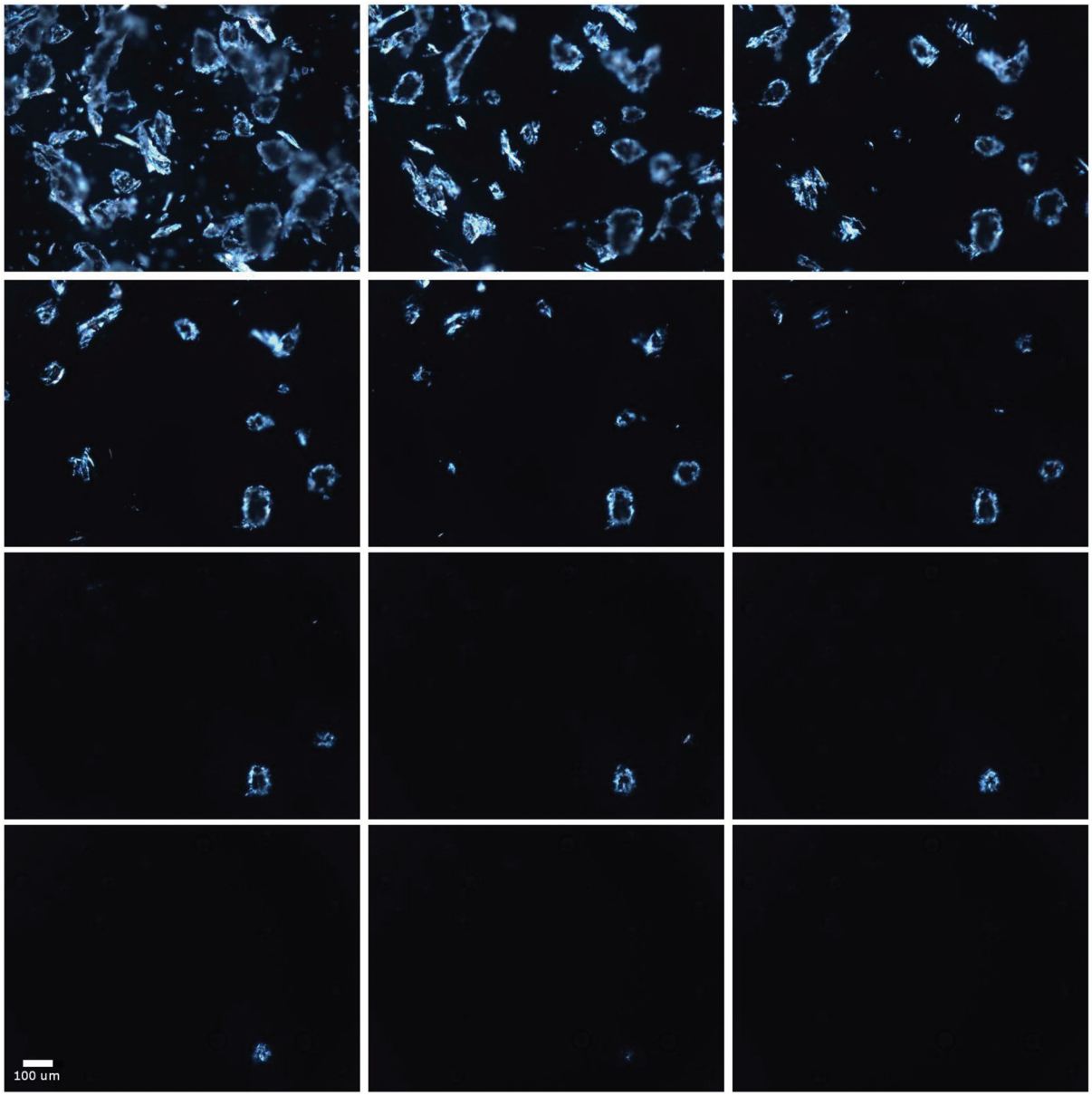

Fig. 2 Images obtained by microscopy under polarized light of 5 wt% cellulose dissolving in $[C_4C_1Im][OAc]$ at 50 °C. MCC fragments appear in white in the images taken after 1, 10, 19, 28, 37 … 91 and 100 minutes (from top left to bottom right).

Fig. 2) and then increases again. This can be attributed to different phenomena: some agglomerates can trap gaseous bubbles (bigger and darker particles shown in some of the snapshots) and, as pictures are taken from the top, agglomerates of particles can hide others; during the dissolution, the agglomerates of cellulose can spread, thus increasing the brightness of the sample. A video of the dissolution processes at 10 wt% at 50 °C showing the release of air bubbles and the increase of the surface taken by agglomerates during their dissolution is given in ESI.†

The possible presence of structural correlation at long distances was scrutinized using low angle X-ray diffraction (2θ limit of 0.7°). The usual cellulose structure was also searched as we covered values of 2θ up to 28°.[35] As shown in Fig. 4, no peak was found at 2θ around 15° and 22.5°, values that are characteristic of microcrystalline cellulose inter-chain organization. This structural organization is apparently replaced by another at longer length scales (corresponding to lower 2θ values). Well-defined diffraction peaks are observed at low angles corresponding to large distance correlations, as high as 12 nm. These sharp peaks indicate a high degree of ordering, *i.e.* large domains of coherence of the composite phase. Arrestingly, for the more intense and single diffraction peak at 2θ = 0.717°, a measured FWHM of 0.013° is indicative of very large size of the associated X-ray coherent domains (in the corresponding diffraction plane here not known) of about half μm (≈ 600 nm). At 2θ = 0.814° two overlapped contributions are observed (2θ = 0.806 and 0.822°) as well as others that are less

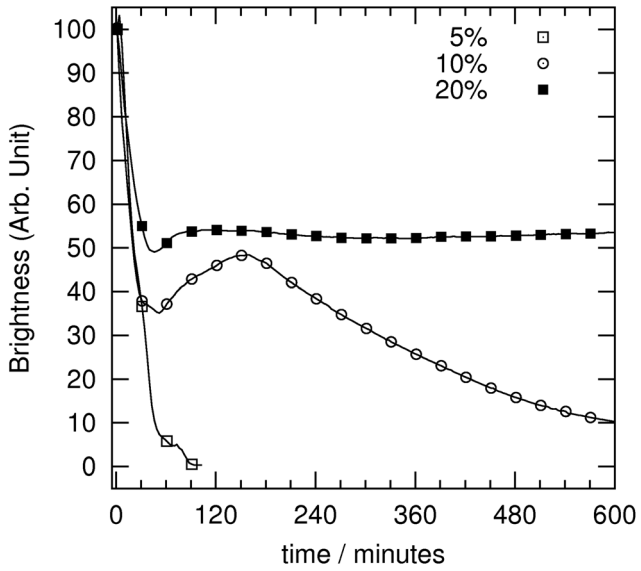

Fig. 3 Dissolution of cellulose at 50 °C as a function of time in solutions of: ⊡ 5 wt% in $[C_4C_1Im][OAc]$; ⊙, 10 wt% in $[C_4C_1Im][OAc]$ and ■, 20 wt% in $[C_4C_1Im][OAc]$.

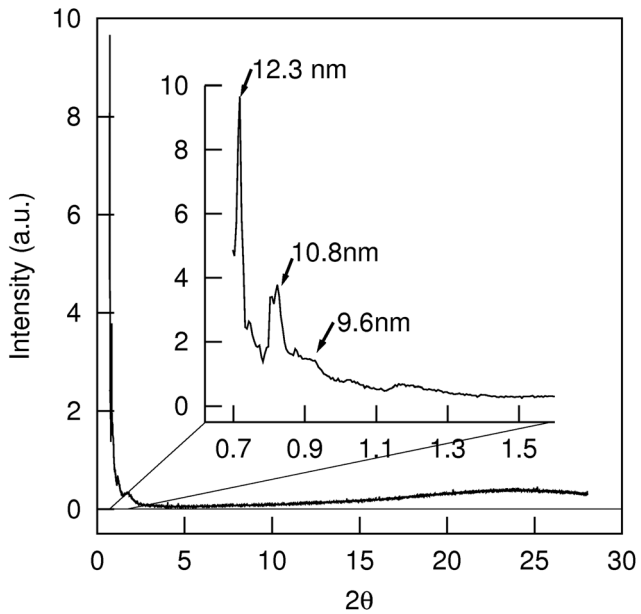

Fig. 4 X-ray diffraction pattern of the ionic liquid + cellulose composite phase.

intense. The observation of the sample under optical polarized-light microscopy, before and after the X-ray analysis, showed no evidence of birefringence (absence of liquid-crystal-type structures), as observed by Song *et al.*[35] for cellulose + $[C_2C_1Im][OAc]$. This suggests that the ordering of the composite phase herein is isotropic, probably three dimensional (bi-dimensional arrangement characterized by harmonic peaks is not depicted here), and adopting a low symmetry (presence of several diffraction peaks).

In order to determine the solubility of cellulose in $[C_4C_1Im][OAc]$ as a function of temperature, we have followed, using the methodology described above, the dissolution of the polymer while heating samples of different mass concentrations at different rates: 0.01, 0.1 and 1 °C min^{-1}. The results are summarized in Fig. 5. For a given heating rate, the temperature of dissolution increases with increasing cellulose concentration and, for a given concentration, increases with increasing heating rate. At temperatures below 100 °C (temperature at which the ionic liquid is known to be decomposed by 1% per 10 hours[23]) up to 25 wt% of cellulose can be dissolved if the sample is heated sufficiently slowly (0.01 °C min^{-1}). This solubility is comparable to what was found in the literature,[9] considering that it strongly depends on the cellulose source and on impurities (such as water or chloride) that can be present in the ionic liquid. Direct comparisons from one study to another are difficult and should be made with care.

The temperatures of the complete dissolution of cellulose are regrouped in Table 1. It can be observed that, when heating at a rate of 1 °C min^{-1}, 5 wt% of cellulose dissolves at 72 °C, while with the slower heating rates of 0.1 and 0.01 °C min^{-1} the temperature of dissolution decreases to 55 °C and 34 °C, respectively. This decrease of the temperature of dissolution is seen for all of the cellulose concentrations and is typical of a solvation process controlled by mass transport. Two different dissolution patterns can, nevertheless, be identified: for the low concentrations of cellulose (5 or 10 wt%) the polymer dissolves at low temperature (around 35 °C) but for higher concentrations of cellulose, part of the polymer dissolves at low temperature, then almost nothing is dissolved up to 70 °C and finally the dissolution restarts to reach complete dissolution between 80 and 95 °C. This result observed in Fig. 5 is in agreement with the results of the dissolution at constant temperature (Fig. 3), where the dissolution of the sample with 20 wt% of cellulose stops around 120 min while the sample with 10 wt% of the polymer continues to dissolve slowly. The cellulose is clearly not dissolving at a constant rate – the first 10 wt% dissolving easier than the remaining solid. These experiments show that, up to around 10 wt% of cellulose, dissolution is accomplished within a few hours at low temperature, while temperatures over 75 °C appear to be necessary in order to dissolve higher concentrations of this polymer.

Adding DMSO to the ionic liquid makes cellulose dissolve much faster and at lower temperatures, as illustrated in Fig. 6 (all experiments using DMSO as a co-solvent were performed using a heating rate of 1 °C min^{-1}). The improvement is negligible when DMSO is added at a concentration of 0.25 mole fraction (or 12 wt%) to $[C_4C_1Im][OAc]$: as in the pure ionic liquid, 5 wt% of cellulose could be dissolved at 70–75 °C. When increasing further the concentration of DMSO (to x_{DMSO} = 0.50 or 28 wt%), we observe the complete dissolution of 5 and 10 wt% of cellulose at temperatures close to 60 °C, in less than 30 min. With x_{DMSO} = 0.75 (54 wt%), complete dissolution of the polymer occurs at a temperature as low as 45 °C (15 min). Temperatures of dissolution obtained for

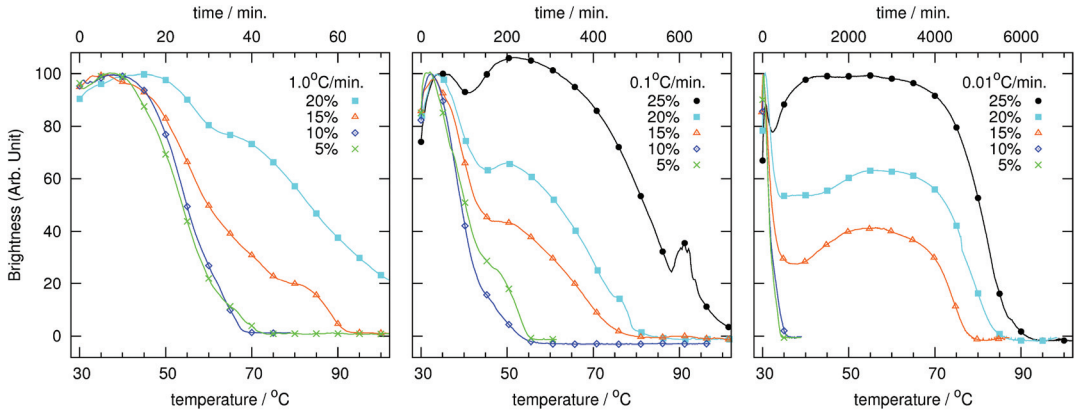

Fig. 5 Dissolution of 5 wt% (×), 10 wt% (◇), 15 wt% (△), 20 wt% (■) and 25 wt% (●) of cellulose in [C_4C_1Im][OAc], as a function of temperature with heating rates of, starting from the left-hand graphic, 1.0, 0.1 and 0.01 °C per minute.

Table 1 Temperature (and time) required for full dissolution of cellulose in [C_4C_1Im][OAc] at different rates: 0.01; 0.1 and 1 °C min^{-1}. In each experiment the sample is heated from 30 to 100 °C

Cellulose	1 °C min^{-1}	0.1 °C min^{-1}	0.01 °C min^{-1}
5 wt%	72 °C (42 min)	55 °C (250 min)	34 °C (400 min)
10 wt%	70 °C (40 min)	52 °C (270 min)	38 °C (800 min)
15 wt%	92 °C (62 min)	72 °C (420 min)	78 °C (4800 min)
20 wt%	X	89 °C (590 min)	84 °C (5400 min)
25 wt%	X	X	90 °C (6000 min)

different concentrations of DMSO and cellulose are given in Table 2. In pure DMSO (x_{DMSO} = 1.0) even 1% of cellulose could not be dissolved. Interestingly, dissolution of cellulose follows the same trend (in terms of kinetics or of the temperature of dissolution) when DMSO is added as a co-solvent or when the heating rate is decreased in the pure ionic liquid. Moreover, it is observed that the addition of DMSO does not have a strong impact on the quantity of cellulose dissolved by an amount of ionic liquid.

Among the broad range of co-solvents tested for the dissolution of cellulose in ionic liquids by Rinaldi,[19] DMSO and DMF (*N*,*N*-dimethylformamide) appear to be the most efficient ones. The ability of organic solvents to swell the cellulose fibers was also recently compared[36] and it was found that microcrystalline cellulose can double in volume when dropped in pure DMSO.[36] The addition of molecular co-solvents to ionic liquids also decreases the viscosity and improves mass-transport substantially.[37] In order to test the hypothesis that the addition of DMSO, a highly polar aprotic solvent, separates the ions of [C_4C_1Im][OAc] and thus improves the dissolution of cellulose,[26] we measured the conductivity of the pure fluids and of the [C_4C_1Im][OAc] + DMSO mixtures between 25 and 100 °C (Fig. 7). We observed that the conductivity of the binary mixtures and of the pure [C_4C_1Im][OAc] increases with increasing temperature. The values given here for the conductivities are higher than the data found in the literature for [C_4C_1Im][OAc],[13,38] as expected since the ionic liquid studied here is doped with 1 wt% of water. The addition of DMSO increases considerably the ionic conductivity for all concentrations and temperatures tested. This increase in conductivity could be

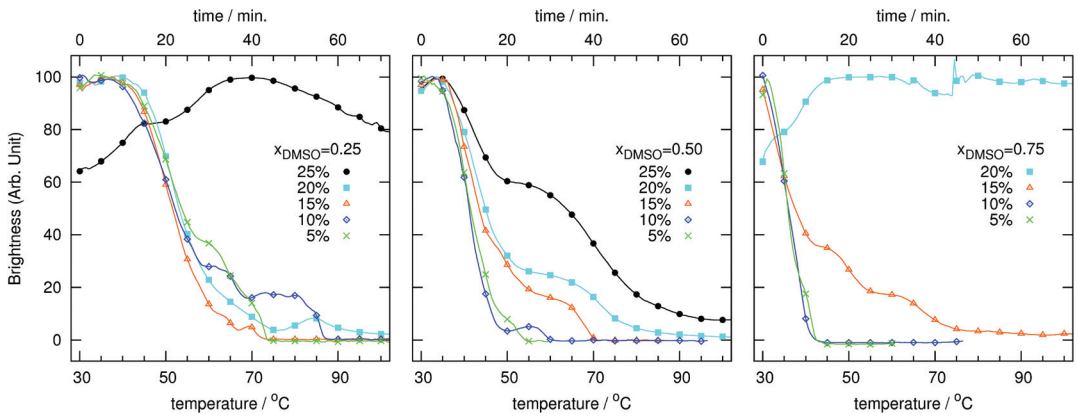

Fig. 6 Dissolution of 5 wt% (×), 10 wt% (◇), 15 wt% (△), 20 wt% (■) and 25 wt% (●) of cellulose in [C_4C_1Im][OAc] + DMSO mixtures, as a function of temperature with a heating rate of 1.0 °C per minute. Mole fraction concentration of DMSO, starting from the left-hand graphic, x_{DMSO} = 0.25, 0.50 and 0.75.

Table 2 Temperature of the full dissolution of cellulose in $[C_4C_1Im]$-[OAc] + DMSO mixtures at different molar concentrations (x_{IL} = 0.25, 0.50 and 0.75) with a heating rate of 1 °C min^{-1} between 30 and 100 °C. The dissolution of 5, 10, 15 and 20 wt% of cellulose (mass of cellulose/mass of solvent) in ionic liquid was tested. The proportion of cellulose compared to the ionic liquid alone is given in parentheses

Cellulose	x_{IL} = 0.25	x_{IL} = 0.50	x_{IL} = 0.75
5 wt%	45 °C (11 wt%)	56 °C (7 wt%)	74 °C (6 wt%)
10 wt%	45 °C (22 wt%)	62 °C (14 wt%)	87 °C (11 wt%)
15 wt%	X (33 wt%)	72 °C (21 wt%)	75 °C (17 wt%)
20 wt%		X (28 wt%)	X (23 wt%)

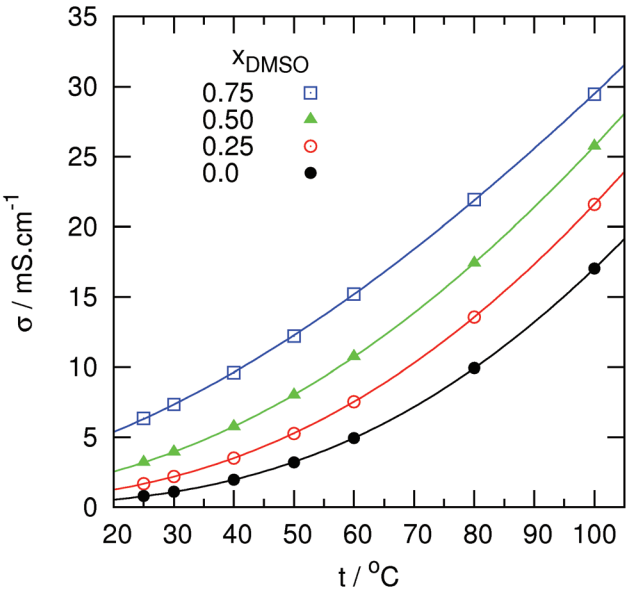

Fig. 7 Electrical conductivity of $[C_4C_1Im][OAc]$ (●) and $[C_4C_1Im][OAc]$ + DMSO mixtures – x_{DMSO} = 0.25 (⊙), 0.50 (▲) and 0.75 (⊡) – as a function of temperature from 25 to 100 °C. Lines correspond to correlations using the VFT equation with parameters reported in ESI.†

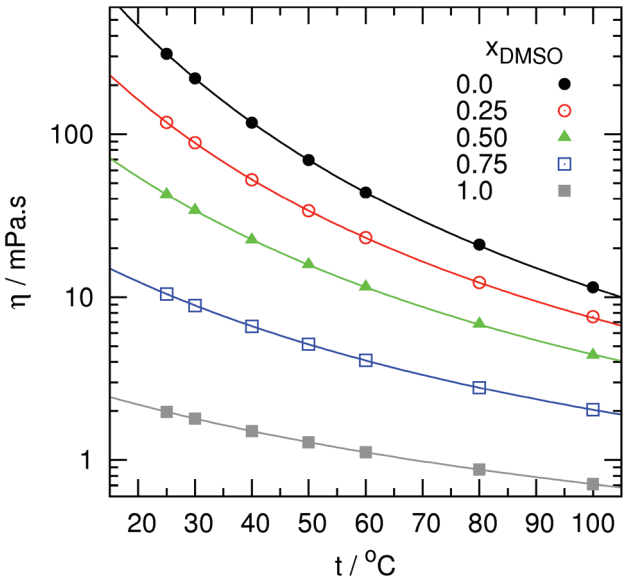

Fig. 8 Viscosity of $[C_4C_1Im][OAc]$ (●), DMSO (■) and $[C_4C_1Im][OAc]$ + DMSO mixtures – x_{DMSO} = 0.25 (⊙), 0.50 (▲) and 0.75 (⊡) – as a function of temperature from 25 to 100 °C. Lines correspond to correlations using the VFT equation with parameters reported in ESI.†

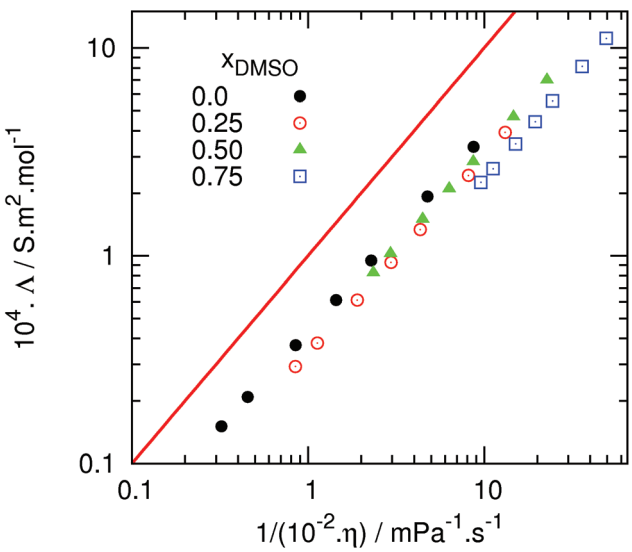

Fig. 9 Walden plot of $[C_4C_1Im][OAc]$ (●) and $[C_4C_1Im][OAc]$ + DMSO mixtures – x_{DMSO} = 0.25 (⊙), 0.50 (▲) and 0.75 (⊡).

due to an increase of the number of ions able to transport charges or to a decrease of the viscosity.

The viscosities of the pure fluids and of the $[C_4C_1Im][OAc]$ + DMSO mixtures were also measured herein and are presented in Fig. 8. Conductivity and viscosity data are given in the ESI.† The viscosity obtained for $[C_4C_1Im][OAc]$ in this work is, as expected, lower than the data found in the literature[13,38] as the ionic liquid is doped with 1 wt% of water.[39] The Walden rule establishes that the product of the molar conductivity and viscosity is constant for dilute electrolyte solutions of weakly coordinating ions in solvents with nonspecific ion–solvent interactions. Data from $[C_4C_1Im][OAc]$ and $[C_4C_1Im][OAc]$ + DMSO mixtures of different compositions are depicted in Fig. 9 as a Walden plot that can be used to provide a qualitative measure of the "ionicity", defined as the effective fraction of ions available to participate in conduction. The reference of ionicity is arbitrarily considered as the line corresponding to an ideal extrapolation of the 0.01 M aqueous KCl solution at 25 °C, which is composed of completely dissociated ions (red line in Fig. 9).[40] Diluted aqueous KCl solutions and mixtures containing ionic liquids are clearly different systems and so the comparisons on the basis of a Walden plot are purely qualitative.[41]

By observing Fig. 9, we can conclude that increasing the amount of DMSO in $[C_4C_1Im][OAc]$ does not increase the ionicity of system under the conditions covered by this work. For the same viscosity, the conductivity tends to decrease slightly when adding the co-solvent (points are more distant from the ideal KCl line). In other words, the addition of DMSO does not increase the number of charge carriers but instead accelerates

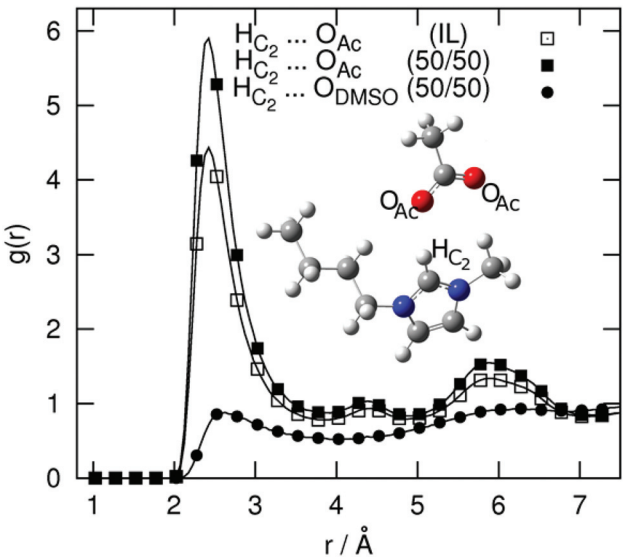

Fig. 10 Site–site radial distribution functions, $g(r)$, between selected sites of the cation, anion and DMSO in pure $[C_4C_1Im][OAc]$ and in $[C_4C_1Im][OAc]$ + DMSO mixtures: ⊡ O_{Ac} around the hydrogen in position C2 of the imidazolium ring in $[C_4C_1Im]$ in the pure ionic liquid; ■, O_{Ac} around the hydrogen in position C2 of the imidazolium ring in $[C_4C_1Im]$ in the equimolar $[C_4C_1Im][OAc]$ + DMSO mixture; ● oxygen atoms of DMSO around the hydrogen in position C2 of the imidazolium ring in $[C_4C_1Im]$ in the equimolar $[C_4C_1Im][OAc]$ + DMSO mixture.

Table 3 Probability of hydrogen bond formation (given in percentage) between the three hydrogen atoms of the imidazolium ring of the cation and the anion in $[C_4C_1Im][OAc]$, calculated by molecular simulation for the pure ionic liquid and when mixed with DMSO

	Without glucose		With glucose	
	$[C_4C_1Im]$-$[OAc]$	$[C_4C_1Im]$-$[OAc]$ + DMSO	$[C_4C_1Im]$-$[OAc]$	$[C_4C_1Im]$-$[OAc]$ + DMSO
$H_{C4,5}$–O_{Ac}	49.0	43.4	48.2	42.0
H_{C2}–O_{Ac}	18.0	17.6	18.1	17.8
$H_{C4,5}$–O_{DMSO}	—	3.0	—	3.1
H_{C2}–O_{DMSO}	—	0.9	—	0.9

Table 4 Probability of hydrogen bond formation (given in percentage) between the anion, the cation and water in the pure ionic liquid and in the $[C_4C_1Im][OAc]$ + H_2O mixtures

	Without glucose		With glucose	
	$[C_4C_1Im]$-$[OAc]$	$[C_4C_1Im]$-$[OAc]$ + H_2O	$[C_4C_1Im]$-$[OAc]$	$[C_4C_1Im]$-$[OAc]$ + H_2O
$H_{C4,5}$–O_{Ac}	49.0	40.2	48.2	38.7
H_{C2}–O_{Ac}	18.0	21.7	18.1	21.3
$H_{C4,5}$–O_{H_2O}	—	14.1	—	13.7
H_{C2}–O_{H_2O}	—	8.3	—	8.1
H_{H_2O}–O_{Ac}	—	171.0	—	164.5
H_{H_2O}–O_{H_2O}	—	6.8	—	8.0

significantly the mass transport as expected: the strong increase of conductivity in the present case is mainly due to a decrease of the viscosity.

The molecular interactions and structure of the $[C_4C_1Im]$-$[OAc]$ + DMSO mixtures were studied by molecular simulation. Examples of the radial distribution function corresponding to the probability of finding the oxygen atoms of the acetate anion or of DMSO close to the hydrogen atom in position C2 of the imidazolium cation are given in Fig. 10. The first peak at 2.4 Å indicates the presence of numerous H-bonds between cations and anions both in the pure ionic liquid and in the $[C_4C_1Im][OAc]$ + DMSO mixtures, an observation already made for $[C_2C_1Im][OAc]$ at lower temperatures.[42] DMSO molecules and acetate anions can accept H-bonds while the imidazolium cation is a H-bond donor mainly *via* the three hydrogen atoms of its aromatic ring. In the $[C_4C_1Im][OAc]$ + DMSO mixtures, DMSO and the anion of the ionic liquid compete to establish H-bonds with the cation, this balance determining the ability of the anion to interact specifically with other molecules such as glucose or cellulose. The radial distribution functions of Fig. 10 show that the presence of DMSO does not perturb the H-bond network of the ionic liquid.

The probability of establishing H-bonds between the three hydrogen atoms of the imidazolium ring of the cation and the anion in $[C_4C_1Im][OAc]$, calculated by molecular simulation, is given in Table 3 for the pure ionic liquid and when mixed with DMSO. Without a co-solvent, almost 50% of the cations interact through H-bonds between the oxygen atoms of the acetate anion and the hydrogen atoms in position 4 or 5 of the imidazolium ring of the cation, $H_{C4,5}$, while less than 20% are bonded by the most acidic hydrogen (H_{C2}) of the imidazolium ring. The number of H-bonds between the anion and the cation ring decreases from 67% to 61% with the addition of DMSO, and the number of H-bonds formed between the cation and DMSO is around fifteen times smaller than that between the two ions. Most of the ionic liquid structure is preserved while adding DMSO, confirming the results found experimentally that show a constant ionicity of the system. In Table 3 are included the probabilities of finding H-bond specific interactions in the presence of glucose, both in the pure $[C_4C_1Im][OAc]$ and in the $[C_4C_1Im][OAc]$ + DMSO mixtures. It is observed that a small amount of glucose has no significant impact on the H-bond network of the ionic liquid.

If DMSO is replaced by a polar protic solvent, for example water at equimolar concentrations, we can observe from the molecular dynamics calculations that water molecules are mainly organized following a (anion···H–O–H···anion) structure, leading to an average of 1.71 and 1.65 H-bond probability between one water molecule and acetate anions (Table 4). This observation (water forming H-bonds simultaneously with two anions at this concentration) agrees with the experimental measurements reported in the literature.[43] Considering that we analyzed equimolar mixtures and that the molar volume of water is smaller than that of DMSO, having a number of H-bonds between anions and cations smaller in the mixture $[C_4C_1Im][OAc]$ + H_2O than in $[C_4C_1Im][OAc]$ + DMSO indicates that H_2O perturbs more the H-bond network of the ionic

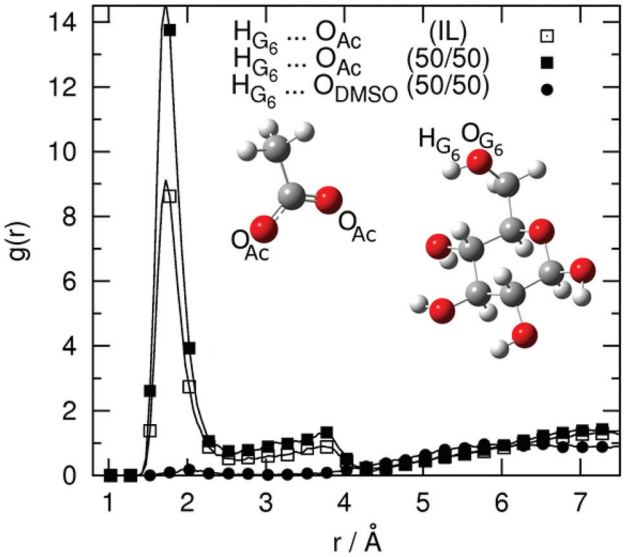

Fig. 11 Site–site radial distribution functions, $g(r)$, between selected sites of glucose and the anion [OAc] or DMSO in solutions of glucose in $[C_4C_1Im][OAc]$ + DMSO mixtures: ⊡ O_{Ac} around the hydrogen in position C6 of glucose (see Fig. 1) in the pure ionic liquid; ■, O_{Ac} around the hydrogen in position C6 of glucose in the equimolar $[C_4C_1Im][OAc]$ + DMSO mixture; ● oxygen atoms of DMSO around the hydrogen in position C6 of glucose in the equimolar $[C_4C_1Im][OAc]$ + DMSO mixture.

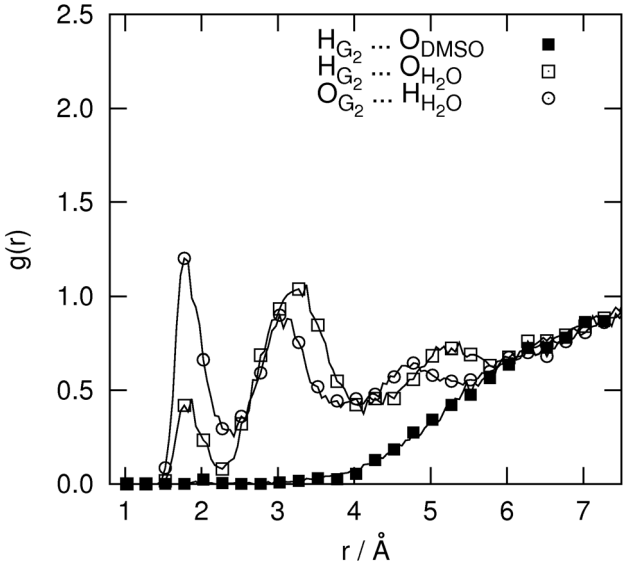

Fig. 12 Site–site radial distribution functions, $g(r)$, between selected sites of glucose and the two co-solvents, water and DMSO: ■, DMSO around the hydrogen in position C2 of glucose (see Fig. 1) in the equimolar $[C_4C_1Im][OAc]$ + DMSO mixture; ⊡, H_2O around the hydrogen in position C2 of glucose in the equimolar $[C_4C_1Im][OAc]$ + H_2O mixture; ⊙, H_2O around the oxygen in position C2 of glucose in the equimolar $[C_4C_1Im][OAc]$ + H_2O mixture.

liquid than DMSO. This is clearly demonstrated by the large probability of formation of H-bonds between H_2O and $C_4C_1Im^+$ (22.4%) when compared with that between DMSO and $C_4C_1Im^+$ (3.9%), as listed in Table 4. Similarly as for DMSO, the addition of glucose molecules has no significant impact on the H-bond network of the ionic liquid.

Glucose is capable of forming H-bonds with $[C_4C_1Im][OAc]$ and with the co-solvent through its five hydroxyl groups that are able to donate or accept H-bonds. Examples of site–site radial distribution functions, calculated by molecular dynamics simulations, are shown in Fig. 11. Radial distribution functions involving other hydroxyl groups of glucose are depicted in the ESI.† The first peak, with a maximum at 1.7 Å, is the typical signature of a strong H-bond here formed most probably between the hydroxyl groups of glucose and the oxygen atoms of the acetate anion of $[C_4C_1Im][OAc]$, both in the pure ionic liquid and in the $[C_4C_1Im][OAc]$ + DMSO mixtures. The probability of existence of H-bonds between glucose and DMSO is low as seen in Fig. 11.

The structure of the $[C_4C_1Im][OAc]$ + H_2O mixtures in the presence of glucose was also studied. The calculated site–site radial distribution functions between selected hydroxyl groups of glucose and atomic sites in water and DMSO are plotted in Fig. 12 (other radial distribution functions are given in the ESI†). It is clearly observed that water can establish H-bonds with glucose, thus competing with the ionic liquid for the same interaction sites, a situation not observed for DMSO since the oxygen atom of DMSO is almost never found within less than 4 Å of a hydrogen atom of glucose. These specific interactions between water and glucose are not enough to promote the dissolution of the biopolymer in this solvent, H_2O being rather used to precipitate cellulose from the ionic liquid solution. This observation was made also by molecular simulation, for example for cellulose in $[C_2C_1Im][OAc]$ where water displaced the ionic liquid's cations out of the first solvation shell of cellulose.[34] Water added at an equimolar ratio (8 wt% of H_2O) competes with the anion of the ionic liquid to form H-bonds with the glucose molecules and so perturbs the specific molecular interactions between glucose and $[C_4C_1Im][OAc]$, decreasing the ability of the ionic liquid to dissolve cellulose. $[C_4C_1Im][Cl]$ with cellulose and either DMSO or water as a co-solvent were also studied recently using the simulation by Huo *et al.*[44] It was found that water molecules were competing with the anion on the cellulose surface while DMSO was only found further in the liquid phase, in agreement with the present results.

The probability of H-bond formation between the glucose hydroxyl groups and the different sites of the $[C_4C_1Im][OAc]$ mixtures is listed in Table 5. The hydrogen bonds involving the hydroxyl groups of glucose as donors and the acetate anion as an acceptor are the most probable (between 88 and 90%), except for the OH group labeled as G6, for which the probability of establishing an H-bond with acetate is lower (around 75%). It is also shown that the oxygen atom in water is accepting H-bonds from glucose around 10 times more than the oxygen atoms in DMSO. Moreover, the addition of water as a co-solvent decreases substantially the probability of the H-bonds between glucose and the anion of the ionic liquid while DMSO does not have a measurable effect (for equimolar concentrations of ionic liquid and co-solvent). It was also

Table 5 Probability of hydrogen bond formation (given in percentage) between glucose and the anion (or co-solvent) in IL–DMSO–glucose and IL–H_2O–glucose simulations

	$[C_4C_1Im]$-[OAc]	$[C_4C_1Im]$-[OAc] + DMSO		$[C_4C_1Im]$-[OAc] + H_2O
H_{G1}–O_{Ac}	89.5	88.0	H_{G1}–O_{Ac}	81.7
H_{G2}–O_{Ac}	88.7	86.6	H_{G2}–O_{Ac}	83.2
H_{G3}–O_{Ac}	88.7	89.2	H_{G3}–O_{Ac}	82.5
H_{G4}–O_{Ac}	89.3	88.4	H_{G4}–O_{Ac}	88.2
H_{G6}–O_{Ac}	75.3	84.2	H_{G6}–O_{Ac}	69.5
H_{G1}–O_{DMSO}	—	0.3	H_{G1}–O_{H_2O}	4.9
H_{G2}–O_{DMSO}	—	0.0	H_{G2}–O_{H_2O}	2.1
H_{G3}–O_{DMSO}	—	0.1	H_{G3}–O_{H_2O}	1.0
H_{G4}–O_{DMSO}	—	0.2	H_{G4}–O_{H_2O}	1.3
H_{G6}–O_{DMSO}	—	0.6	H_{G6}–O_{H_2O}	5.3

observed that water molecules act preferentially as H-bond receptors for the glucose molecules than as H-bond donors. These results agree well with the study of Huo *et al.* on the interface between cellulose and $[C_4C_1Im]Cl$ plus DMSO or water as a co-solvent.[34,44]

Zhao *et al.*[26] reported recently a molecular simulation study of the effect of co-solvents on the interactions between $[C_4C_1Im][OAc]$ and cellulose, including DMSO and water. In their study the molar ratio of DMSO/ionic liquid is significantly higher than here (R = 2.54 compared to R = 1 in the present work). Also, herein are obtained by simulation mainly structural quantities such as H-bond statistics and radial distribution functions, which give a detailed picture of the spatial correlations between specific interaction sites, whereas Zhao *et al.* report energetic quantities, which are more global. These authors observe a larger effect of DMSO on the cation–anion interactions, compatible with the difference in molar ratio. The observations on the effect of water reducing the anion–cellulose interactions reported by Zhao *et al.*[26] agree with the conclusions of this work.

4. Conclusions

Cellulose dissolution in $[C_4C_1Im][OAc]$ (with a constant 1 wt% water) and in $[C_4C_1Im][OAc]$ + DMSO mixtures was studied experimentally from 30 to 100 °C using a synthetic phase equilibrium method based on polarized microscopy. The brightness of the microscope images was quantified and could be used to qualitatively assess the evolution of the dissolution of the biopolymer. A quantitative analysis was difficult due to non-controlled changes in the brightness of the sample during the dissolution. The complete dissolution of cellulose could be determined reproducibly using this technique.

Up to 10 wt% of cellulose could be dissolved at temperatures below 40 °C within a few hours, while higher concentrations of cellulose (up to 25 wt%) were dissolved at temperatures above 75 °C. Addition of DMSO as a co-solvent allows a much faster dissolution of cellulose – up to 10 wt% within 15 minutes at 45 °C. This faster dissolution can be explained here, as for other polymers in different solvents, by a decrease in the viscosity of the medium as no increase in the ionicity (anion–cation dissociation) of the ionic liquid solutions was observed experimentally and, by molecular simulation, only a small decrease of the probability of cation–anion H-bond formation was obtained for glucose solutions.

The structure and molecular interactions of the glucose solutions were assessed by molecular simulation. It is confirmed that the mechanism of glucose dissolution in the acetate-based ionic liquid involves the formation of a new H-bond network between the anions and the solute. The addition of DMSO does not affect significantly the ionic liquid–glucose interactions, indicating that this molecular co-solvent enables the dissolution of cellulose by facilitating mass transport in the fluid. The same results were not found for water as a co-solvent. In this case, H_2O participates in the H-bond network of the solvent and, in the presence of glucose, competes with the anion to form H-bonds with glucose. This might have caused the precipitation of the polymer upon addition of water.

Acknowledgements

J.-M.A. is financed by the Contrat d'Objectifs Partagés, CNRS-UBP-Région Auvergne, France.

References

1 A. J. Ragauskas, C. K. Williams, B. H. Davison, G. Britovsek, J. Cairney, C. A. Eckert, W. J. Frederick, J. P. Hallett, D. J. Leak, C. L. Liotta, J. R. Mielenz, R. Murphy, R. Templer and T. Tschaplinski, *Science*, 2006, **311**, 484–489.
2 M. Gericke, P. Fardim and T. Heinze, *Molecules*, 2012, **17**, 7458–7502.
3 T. Liebert, in *Cellulose Solvents: For Analysis, Shaping and Chemical Modification*, American Chemical Society, 2010, vol. 1033, ch. 1, pp. 3–54.
4 R. P. Swatloski, S. K. Spear, J. D. Holbrey and R. D. Rogers, *J. Am. Chem. Soc.*, 2002, **124**, 4974–4975.
5 N. V. Plechkova and K. R. Seddon, *Chem. Soc. Rev.*, 2008, **37**, 123–150.
6 A. Pinkert, K. N. Marsh, S. Pang and M. P. Staiger, *Chem. Rev.*, 2009, **109**, 6712–6728.
7 Y. Fukaya, A. Sugimoto and H. Ohno, *Biomacromolecules*, 2006, **7**, 3295–3297.
8 M. E. Zakrzewska, E. Bogel-Łukasik and R. Bogel-Łukasik, *Energy Fuels*, 2010, **24**, 737–745.
9 B. Zhao, L. Greiner and W. Leitner, *RSC Adv.*, 2012, **2**, 2476–2479.
10 B. Kosan, C. Michels and F. Meister, *Cellulose*, 2008, **15**, 59–66.
11 A. Xu, J. Wang and H. Wang, *Green Chem.*, 2010, **12**, 268–275.

12 R. L. Gardas and J. A. P. Coutinho, *Fluid Phase Equilib.*, 2008, **266**, 195–201.
13 A. Xu, Y. Zhang, Z. Li and J. Wang, *J. Chem. Eng. Data*, 2012, **57**, 3102–3108.
14 M. Gericke, K. Schlufter, T. Liebert, T. Heinze and T. Budtova, *Biomacromolecules*, 2009, **10**, 1188–1194.
15 R. Sescousse, K. A. Le, M. E. Ries and T. Budtova, *J. Phys. Chem. B*, 2010, **114**, 7222–7228.
16 C. S. Lovell, A. Walker, R. A. Damion, A. Radhi, S. F. Tanner, T. Budtova and M. E. Ries, *Biomacromolecules*, 2010, **11**, 2927–2935.
17 H. Cruz, M. Fanselow, J. D. Holbrey and K. R. Seddon, *Chem. Commun.*, 2012, **48**, 5620–5622.
18 B. Lindman, G. Karlström and L. Stigsson, *J. Mol. Liq.*, 2010, **156**, 76–81.
19 R. Rinaldi, *Chem. Commun.*, 2011, **47**, 511–513.
20 A. Xu, Y. Zhang, Y. Zhao and J. Wang, *Carbohydr. Polym.*, 2013, **92**, 540–544.
21 Y. Lv, J. Wu, J. Zhang, Y. Niu, C.-Y. Liu, J. He and J. Zhang, *Polymer*, 2012, **53**, 2524–2531.
22 M. Iguchi, K. Kasuya, Y. Sato, T. Aida, M. Watanabe and R. Smith Jr., *Cellulose*, 2013, **20**, 1353–1367.
23 A. Brandt, J. Grasvik, J. P. Hallett and T. Welton, *Green Chem.*, 2013, **15**, 550–583.
24 M. FitzPatrick, P. Champagne, M. F. Cunningham and C. Falkenburger, *Can. J. Chem. Eng.*, 2012, **90**, 1142–1152.
25 M. Zavrel, D. Bross, M. Funke, J. Büchs and A. C. Spiess, *Bioresour. Technol.*, 2009, **100**, 2580–2587.
26 Y. Zhao, X. Liu, J. Wang and S. Zhang, *J. Phys. Chem. B*, 2013, **117**, 9042–9049.
27 J. N. Canongia Lopes, M. F. Costa Gomes, P. Husson, A. l. A. H. Pádua, L. P. N. Rebelo, S. Sarraute and M. Tariq, *J. Phys. Chem. B*, 2011, **115**, 6088–6099.
28 W. L. Jorgensen, D. S. Maxwell and J. Tirado-Rives, *J. Am. Chem. Soc.*, 1996, **118**, 11225–11236.
29 J. N. Canongia Lopes, J. Deschamps and A. A. H. Pádua, *J. Phys. Chem. B*, 2004, **108**, 2038–2047.
30 J. Canongia Lopes and A. H. Pádua, *Theor. Chem. Acc.*, 2012, **131**, 1–11.
31 W. Damm, A. Frontera, J. Tirado–Rives and W. L. Jorgensen, *J. Comput. Chem.*, 1997, **18**, 1955–1970.
32 W. L. Jorgensen, J. Chandrasekhar, J. D. Madura, R. W. Impey and M. L. Klein, *J. Chem. Phys.*, 1983, **79**, 926–935.
33 W. Smith and T. Forester, *J. Mol. Graphics*, 1996, **14**, 136–141.
34 H. Liu, K. L. Sale, B. A. Simmons and S. Singh, *J. Phys. Chem. B*, 2011, **115**, 10251–10258.
35 H. Song, Y. Niu, Z. Wang and J. Zhang, *Biomacromolecules*, 2011, **12**, 1087–1096.
36 L. C. Fidale, N. Ruiz, T. Heinze and O. A. E. Seoud, *Macromol. Chem. Phys.*, 2008, **209**, 1240–1254.
37 A. Stoppa, J. Hunger and R. Buchner, *J. Chem. Eng. Data*, 2008, **54**, 472–479.
38 J. Araújo, A. Pereiro, F. Alves, I. Marrucho and L. Rebelo, *J. Chem. Thermodyn.*, 2013, **57**, 1–8.
39 S. Fendt, S. Padmanabhan, H. W. Blanch and J. M. Prausnitz, *J. Chem. Eng. Data*, 2010, **56**, 31–34.
40 W. Xu, E. I. Cooper and C. A. Angell, *J. Phys. Chem. B*, 2003, **107**, 6170–6178.
41 C. Schreiner, S. Zugmann, R. Hartl and H. J. Gores, *J. Chem. Eng. Data*, 2009, **55**, 1784–1788.
42 D. T. Bowron, C. D'Agostino, L. F. Gladden, C. Hardacre, J. D. Holbrey, M. C. Lagunas, J. McGregor, M. D. Mantle, C. L. Mullan and T. G. A. Youngs, *J. Phys. Chem. B*, 2010, **114**, 7760–7768.
43 L. Cammarata, S. G. Kazarian, P. A. Salter and T. Welton, *Phys. Chem. Chem. Phys.*, 2001, **3**, 5192–5200.
44 F. Huo, Z. Liu and W. Wang, *J. Phys. Chem. B*, 2013, **117**, 11780–11792.

